

Assessment of FY-3A and FY-3B MWHS observations

Keyi Chen^{1,2,3}, Stephen English,
Niels Bormann and Jiang Zhu¹

Research Department

September 2014

¹ International Center for Climate and Environment Sciences, Institute of Atmospheric Physics, China.

² University of Chinese Academy of Sciences.

³ The Department of Atmospheric Sciences, Chengdu University of Information & Technology.

This paper has not been published and should be regarded as an Internal Report from ECMWF.
Permission to quote from it should be obtained from the ECMWF.



Series: ECMWF Technical Memoranda

A full list of ECMWF Publications can be found on our web site under:

<http://www.ecmwf.int/en/research/publications>

Contact: library@ecmwf.int

© Copyright 2014

European Centre for Medium-Range Weather Forecasts

Shinfield Park, Reading, Berkshire RG2 9AX, England

Literary and scientific copyrights belong to ECMWF and are reserved in all countries. This publication is not to be reprinted or translated in whole or in part without the written permission of the Director-General. Appropriate non-commercial use will normally be granted under the condition that reference is made to ECMWF.

The information within this publication is given in good faith and considered to be true, but ECMWF accepts no liability for error, omission and for loss or damage arising from its use.

Abstract

The FY-3 series began in May 2008 with the launch of the FY-3A satellite. The Microwave Humidity Sounders (MWHS) provide vertical information about water vapour, which is important for numerical weather prediction (NWP). The Noise Equivalent Delta Temperature (NEDT) of the MWHS is higher than that of the Microwave Humidity Sounder (MHS) instrument (e.g. on MetOp-B) but lower than that of the older AMSU-B instruments (on NOAA-15, 16 and 17). Assimilation of MWHS observations into the ECMWF Integrated Forecasting System (IFS) improved the fit of short-range forecasts to other observations, notably MHS, and also slightly improved the longer-range forecast scores verified against analysis. Also, assimilating both the MWHS/FY-3A and the MWHS/FY-3B gave a larger impact than either instrument alone. Although some minor negative impacts were found, originating in the Tropics, the quality control appears to be adequate for a successful assimilation of MWHS. Substitution trials indicate that MWHS/FY-3 series data can recover a large proportion of the impact of a similar number of MHS data. These encouraging results suggest that the FY-3 series MWHS data has the quality required for use in NWP assimilation systems and can be implemented at ECMWF.

1 Introduction

China launched the first FY-3 satellite in May 2008. This was the second generation of the Chinese polar-orbiting satellites, carrying significantly more sophisticated sensors for operational meteorology than the first generation. The first two satellites in the series, FY-3A and FY-3B, were classed as research satellites. In September 2013, the third satellite (FY-3C) was launched as the first operational satellite. The microwave instruments onboard have the potential to play an important role in numerical weather prediction (NWP). Therefore, a detailed assessment of the data quality of these microwave radiometers on the preparatory FY-3 satellites is required.

Since the FY-3 series is expected to become an important data source for NWP, reanalysis and climate sciences, this assessment has already begun. Lu et al. (2011a) assessed the microwave temperature sounder (MWTS) against a baseline of the operational ECMWF NWP short-range forecast, using the RTTOV radiative transfer model (Saunders et al. 1999). Significant biases were found and it was suggested that these were related both to shifts in the frequency of the channel pass-bands and to radiometer non-linearity. After these effects were properly accounted for, the data quality of MWTS and MWHS was found to be broadly comparable with AMSU-A and MHS in terms of bias (Zou et al. 2011). Observing system experiments suggested that the impacts were neutral to slightly positive, which was encouraging and built confidence that the following series of the FY-3 instruments would be widely used in NWP data assimilation systems (Lu et al. 2011a). The studies to date focused primarily on the MWTS. In this study the focus is on the humidity sounder, the MWHS.

In section 2, the microwave humidity sounders from FY-3 series and MetOp-B are described and compared; section 3 presents the data quality assessment based on statistical analysis of the first-guess departures; the data assimilation experiments are described in section 4 and section 5. Conclusions are presented in section 6.

2 Microwave humidity sounders

2.1 MWHS data

The FY-3 series MWHS is a five-channel cross-track scanning instrument able to provide vertical humidity information to the NWP data assimilation systems. The vertical resolution is poor, with only 2 to 3 pieces of independent information. Nonetheless, this has been proven valuable to NWP in the past. The central frequencies of MWHS are shown in Table 1. It measures microwave radiation at five channels: 150GHz (V), 150GHz (H), 183.31±1GHz (V), 183.31±3GHz (V) and 183.31±7GHz (V). The nominal spatial resolution is 15km at nadir and the swath width is 2700km with a total of 98 FOVs (field of view) along each scan-line (Table 2).

Channel number		Frequency (GHz)		Bandwidth (MHz)	
MHS	MWHS	MHS	MWHS	MHS	MWHS
1	1	89(V)	150(V)	1400×2	1000×2
2	2	157(V)	150(H)	1400×2	1000×2
3	3	183.31±1(H)	183.31±1(V)	500×2	500×2
4	4	183.31±3(H)	183.31±3(V)	1000×2	1000×2
5	5	190.31(V)	183.31±7(V)	1000×2	1000×2

Table 1. MHS and MWHS channel characteristics

2.2 MHS data

The MHS data used in this report is from the MetOp-B satellite. MHS is also a cross-track scanning microwave radiometer. It also has five channels, but with slightly different frequencies to the MWHS: 89GHz (V), 157GHz (V), 183.31±1GHz (H), 183.31±3GHz (H) and 190.31 (V). The nominal spatial resolution is the same as MWHS at nadir, but the swath width is smaller than MWHS, only 2250km, with a total of 90 FOVs along each scan-line (Table 2). This means that in the Tropics MWHS has smaller gaps between consecutive orbits than MHS.

Channel number		Nadir res. (km)		Peak of weighting function (WF) (hPa)		Swath width (km)	
MHS	MWHS	MHS	MWHS	MHS	MWHS	MHS	MWHS
1	1	15	15	surface	surface	2250	2700
2	2	15	15	surface	surface	2250	2700
3	3	15	15	400	400	2250	2700
4	4	15	15	600	600	2250	2700
5	5	15	15	800	800	2250	2700

Table 2. MHS and MWHS channel characteristics

3 Data quality assessment

Figure 1 compares the MWHS and the corresponding MHS channel 3 fit to the ECMWF short-range forecast and analysis. In these plots the statistics for all data are plotted (i.e. including data that does not pass quality control checks). The standard deviation of the first-guess departure (O-B) of the MWHS is

larger, and with larger variations with time, than that of the MHS (Fig. 1 (a)-(b)). The number of MWHS observations available also varies more than is found for MHS (Fig. 1 (c)-(d)).

In order to decrease the geophysical noise, a dataset was defined based on a criterion that the first-guess departures of channel 1 are below 5K. This is to remove observations strongly affected by ice cloud and precipitation, so the dataset is referred to as “clear data”. The clear data of MWHS is compared with the MHS data that passes quality control tests for assimilation in the ECMWF forecasting system, which is called “used data”. Also, since the emissivity of the land is more complex, the data is compared only over sea (Figure 2). A spike occurred on 10th July in the time series of the standard deviation of the first-guess departure (O-B) of the MWHS, while no such kind of spike appears in the MHS used data.

This spike clearly relates to an anomaly in the MWHS data. The first-guess departures with the absolute value larger than 15K on the spike day (July 10th, 2013) are plotted in Figure 3 and show that this occurred for a small number of scan lines, suggesting an error in the calibration. However, with the data available it is not possible to diagnose why the calibration was wrong for these scan lines.

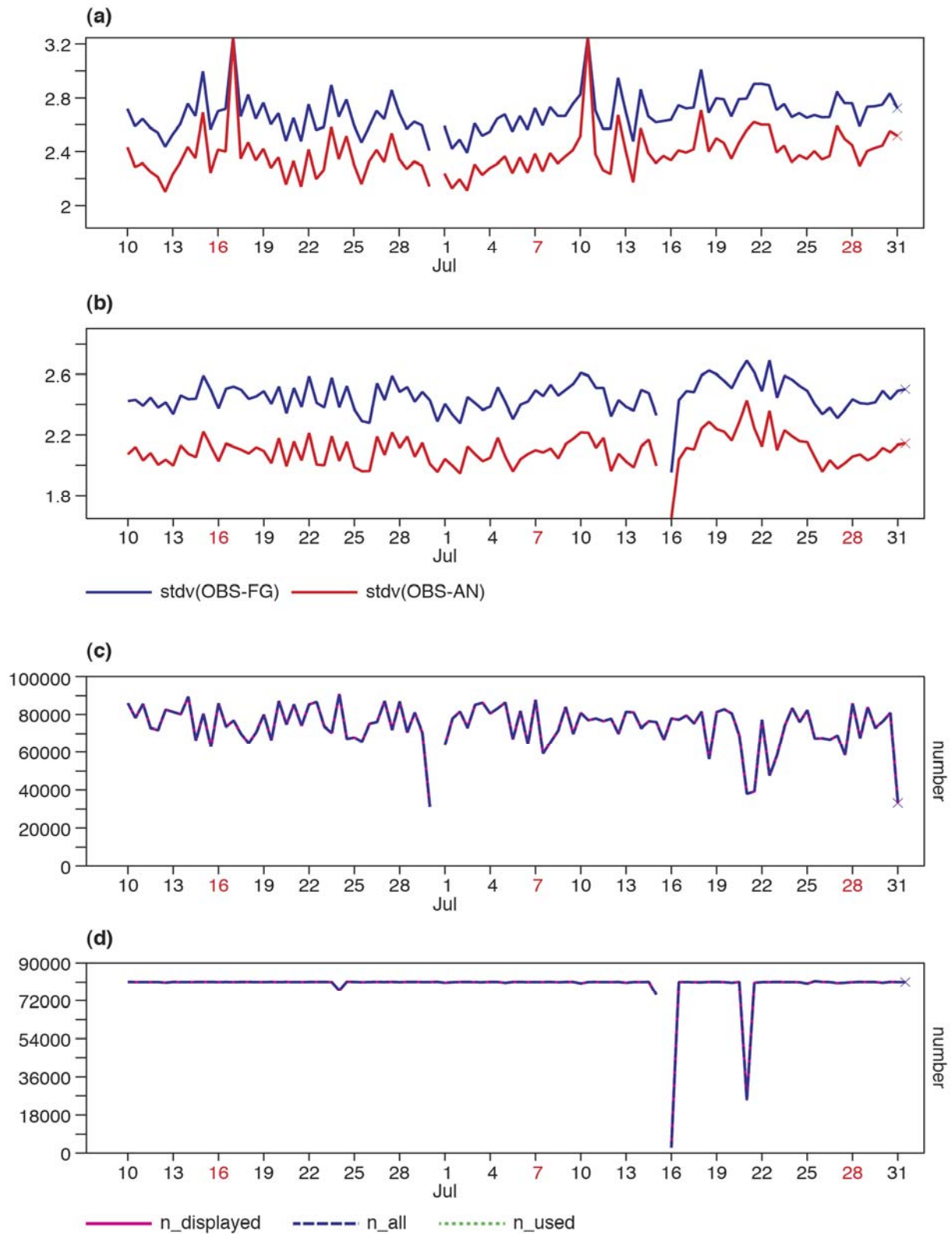


Figure 1. (a) time series of the standard deviation of the first-guess departure (O-B) of the MWS channel 3 for all data; (b) time series of the standard deviation of the first-guess departure (O-B) of MWS channel 3 for all data; (c) time series of the 6-hourly sample number of the MWS; (d) time series of the 6-hourly sample number of MWS.

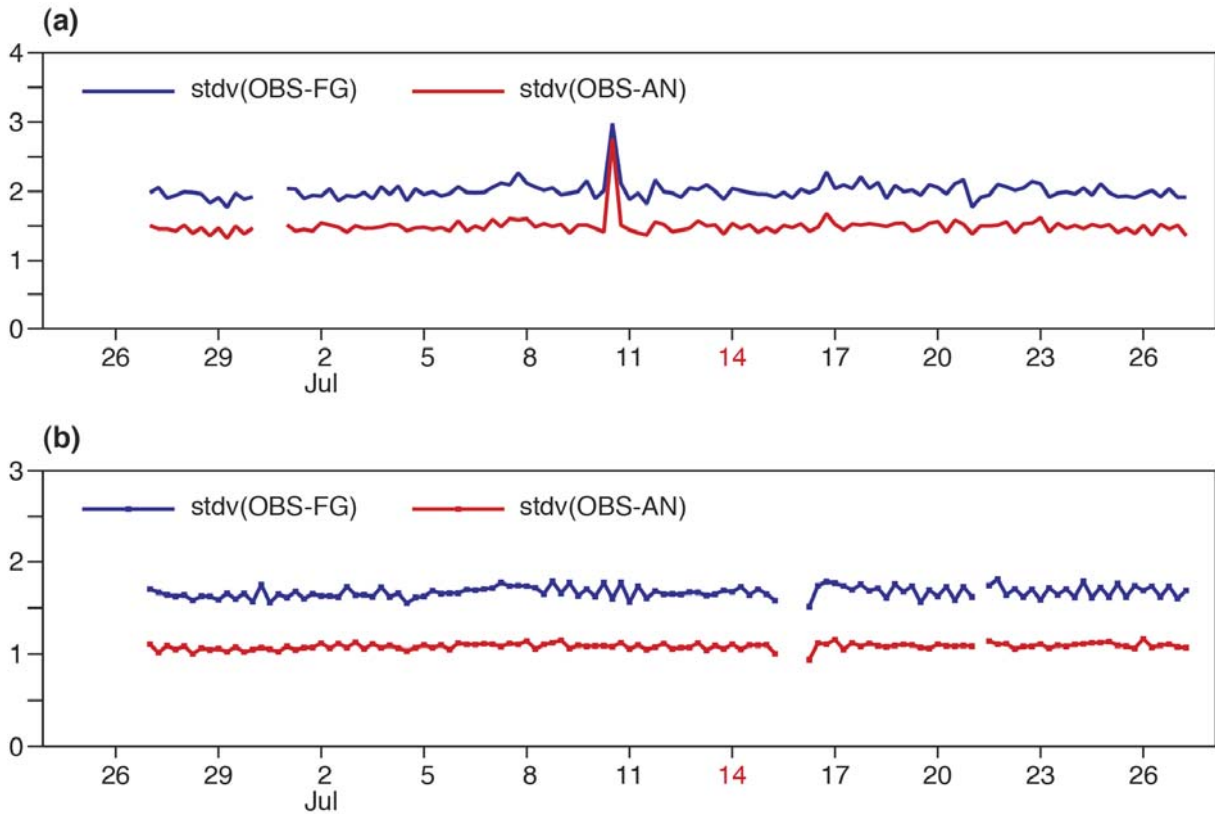


Figure 2. (a) the time series of the standard deviation of the first-guess departure (O-B) of the MWHS channel 3 for clear data over sea; (b) the time series of the standard deviation of the first-guess departure (O-B) of MHS channel 3 for used data over sea.

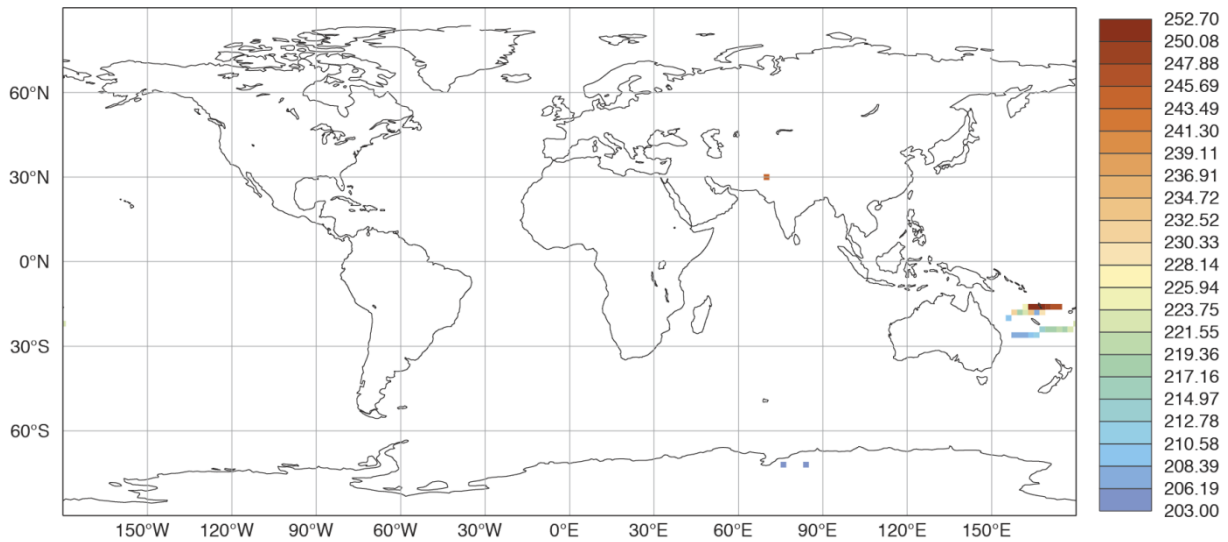


Figure 3. Locations of the first-guess departures with the absolute value larger than 15K on July 10th, 2013.

4 Data assimilation experiments

4.1 Summer trial experiments set-up

As the monitoring showed that, in general, MWHS data is of good quality, the MWHS data has been experimentally assimilated into the ECMWF forecasting system (IFS). As explained in section 3 only clear data over sea is used.

To remove redundant satellite observations and to reduce the impact of spatial error correlations, spatial thinning is performed and the best quality data is retained. An average distance of about 140km is applied. Data contaminated by significant cloud or rain signals is also removed before being supplied to the 4D-Var minimization in the clear-sky assimilation scheme, using the window channel check developed in the previous section. Variational bias correction (VarBC, Dee, 2004) is applied to the observations, as has been done for all microwave radiances in the IFS since Cycle 31r1. This accounts for possible systematic errors in selected observations and/or observation operators. The systematic errors (or biases) are represented by linear predictor models, which can be formulated separately for different groups of observations. Observational errors are assigned to MHS and MWHS as shown in the following table:

MWHS observation errors			MHS observation errors		
CH3	CH4	CH5	CH3	CH4	CH5
2.3K	2.5K	2.4K	2K	2K	2K

Table 3. Assigned observation errors of MWHS and MHS

One control and three experiments are run to test the impact of MWHS assimilation, using ECMWF Cycle 38r2 with a T511 spectral truncation, corresponding to a spatial resolution of around 40km. The control (Exp ID is fz1w) was run from July 10th, 2013 to September 10th, 2013 and forecast times are 00Z and 12Z each day, which provides 125 forecast samples in total. The control run assimilates the same observations used operationally by ECMWF on these dates i.e. excluding MWHS. The first experiment added the MWHS on FY-3A (ID fz1u). The second experiment added the MWHS on FY-3B with the experiment period from July 7th, 2013 to September 7th, 2013. The IDs are fz1y and fz1z for control and experiment respectively. The third experiment (Exp ID is fzc0) added both the MWHS/FY-3A and MWHS/FY-3B into the assimilation system at the same time with the same experiment period.

4.2 MWHS used data assessment

After assimilation, the probability density functions of the first-guess departure of MWHS and MHS are compared (Figure 4). The MWHS data (blue line) has higher noise than MHS (red line). To quantify this, artificial random noise is added to each channel of MHS (only channel 3 figures are shown). The two curves fit with each other after 0.8K and 1K of random noise are added separately to CH3 of MHS in order to compare with MWHS/FY-3A and MWHS/FY-3B, respectively. The random noise values are broadly consistent with the NEDT mentioned in the previous studies (Zou et al. 2011, Lu et al. 2011b).

Figure 5 indicates that the quality control (QC) employed in the IFS removes the badly calibrated scan lines identified in section 3. This is mainly achieved by the “First Guess” check that rejects data that deviates too much from the first guess. The time series of MWHS is much smoother than that in Figure 2, but because MWHS has more noise, the value of the standard deviation of the first-guess departure and its variation with time are still larger than for MHS. It is very interesting to notice that after assimilation, the MWHS 6-hour sample number varies like a wave-shape with time, while the MHS sample number does not. This is due to the assimilation priority of MHS. Therefore, if MWHS data has the overlap in space and time with MHS data, only MHS is used to eliminate data redundancy. The date (00Z, August 10th, 2013) with the least MWHS used sample is picked out and sample distributions of MWHS and MHS are displayed in Figure 6. Obviously, the missing sample of MWHS overlapped with MHS in space and time and the MWHS sample number variation period with time depends on the time difference between MWHS and MHS.

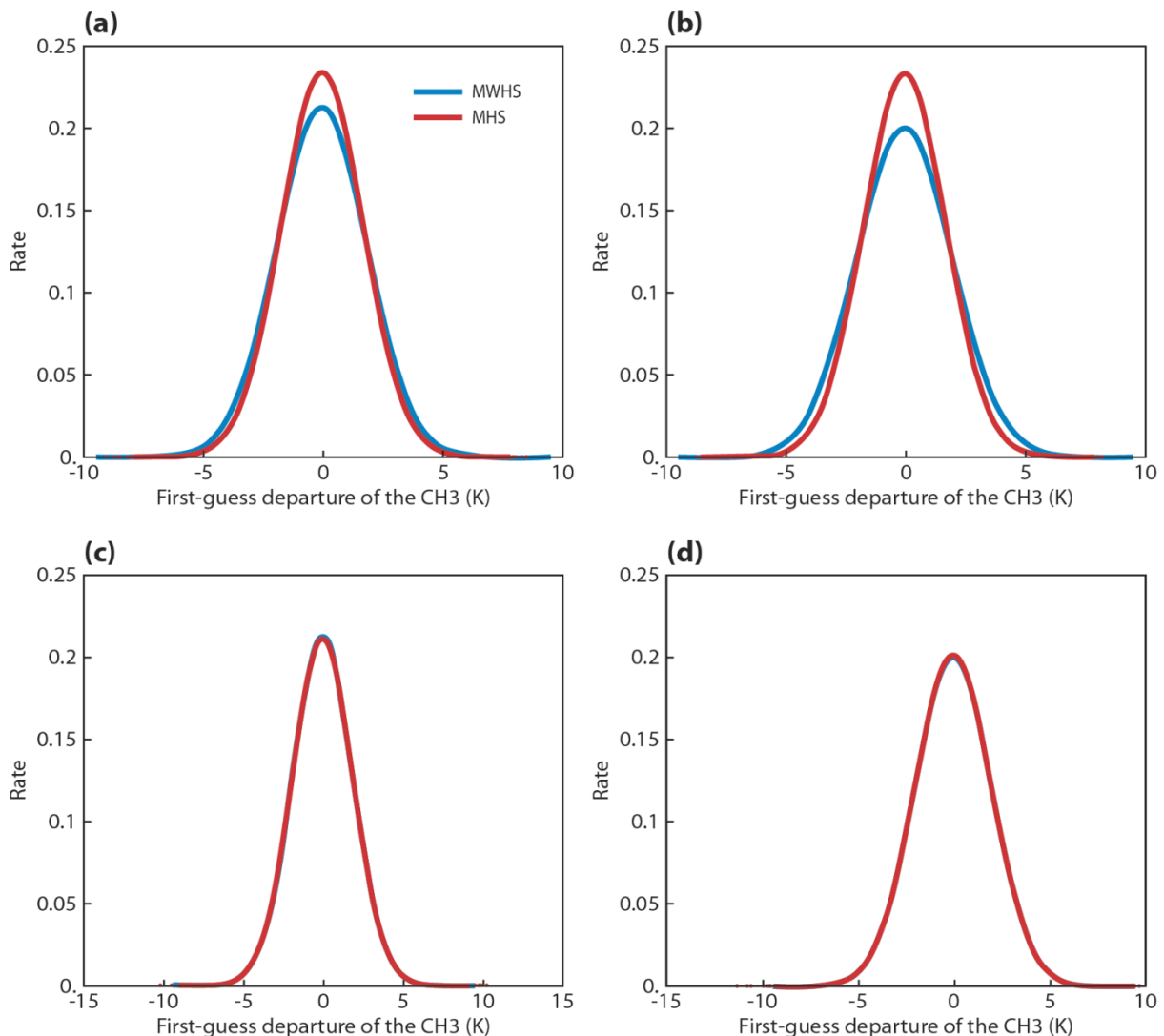


Figure 4. The probability density functions of the first-guess departure of MWHS and MHS. (a) MWHS/FY-3A (blue) vs. MHS (red); (b) MWHS/FY-3B (blue) vs. MHS (red); (c) MWHS/FY-3A (blue) vs. MHS (red) with random noise 0.8K added; (d) MWHS/FY-3B (blue) vs. MHS (red) with random noise 1K added.

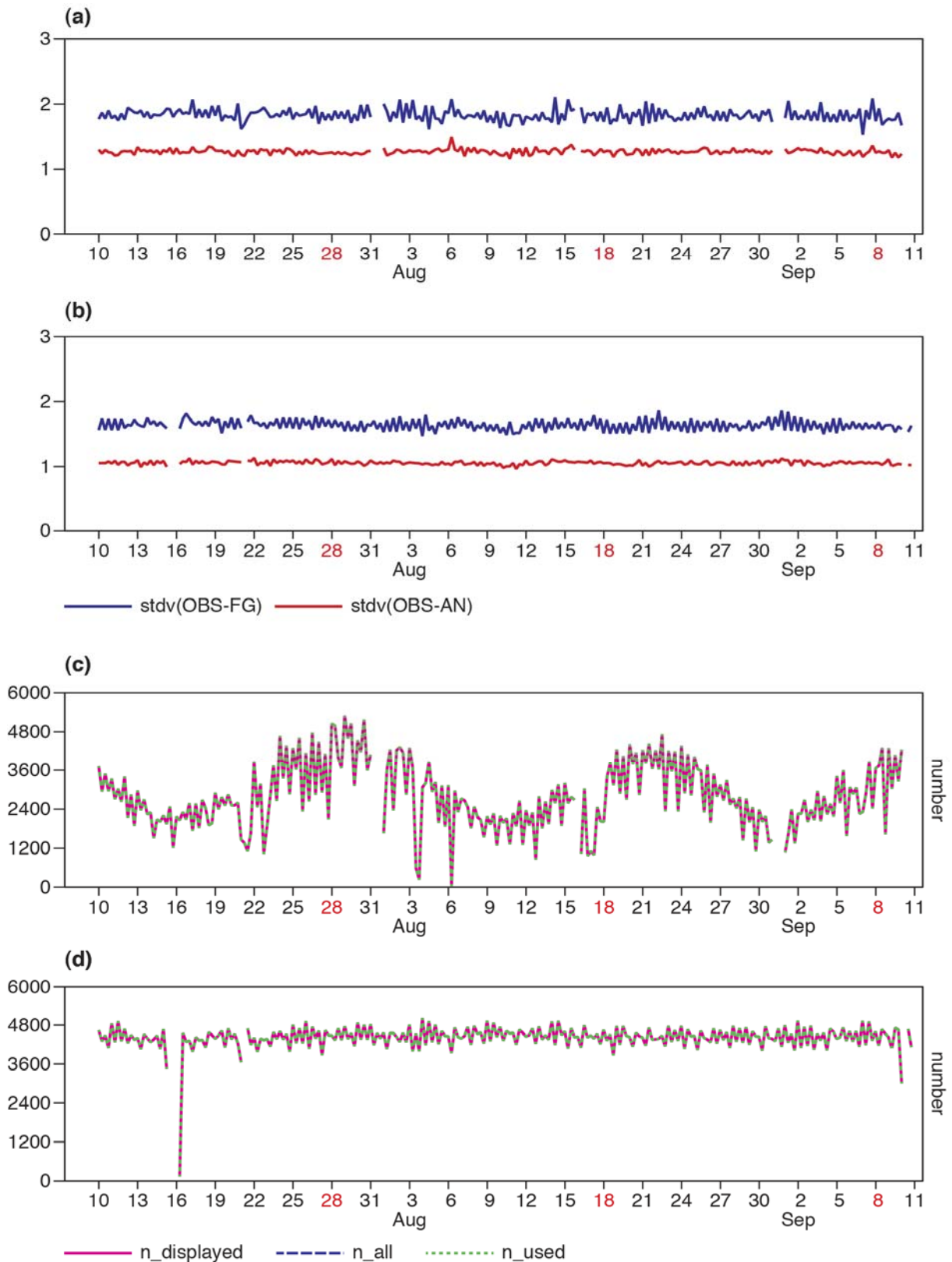


Figure 5. (a) the time series of the standard deviation of the first-guess departure (O-B) of the MWHS in channel 3 for used data over sea; (b) the time series of the standard deviation of the first-guess departure (O-B) of the MHS in channel 3 for used data over sea; (c) the time series of the 6-hourly sample number of the MWHS used data; (d) the time series of the 6-hourly sample number of MHS used data.

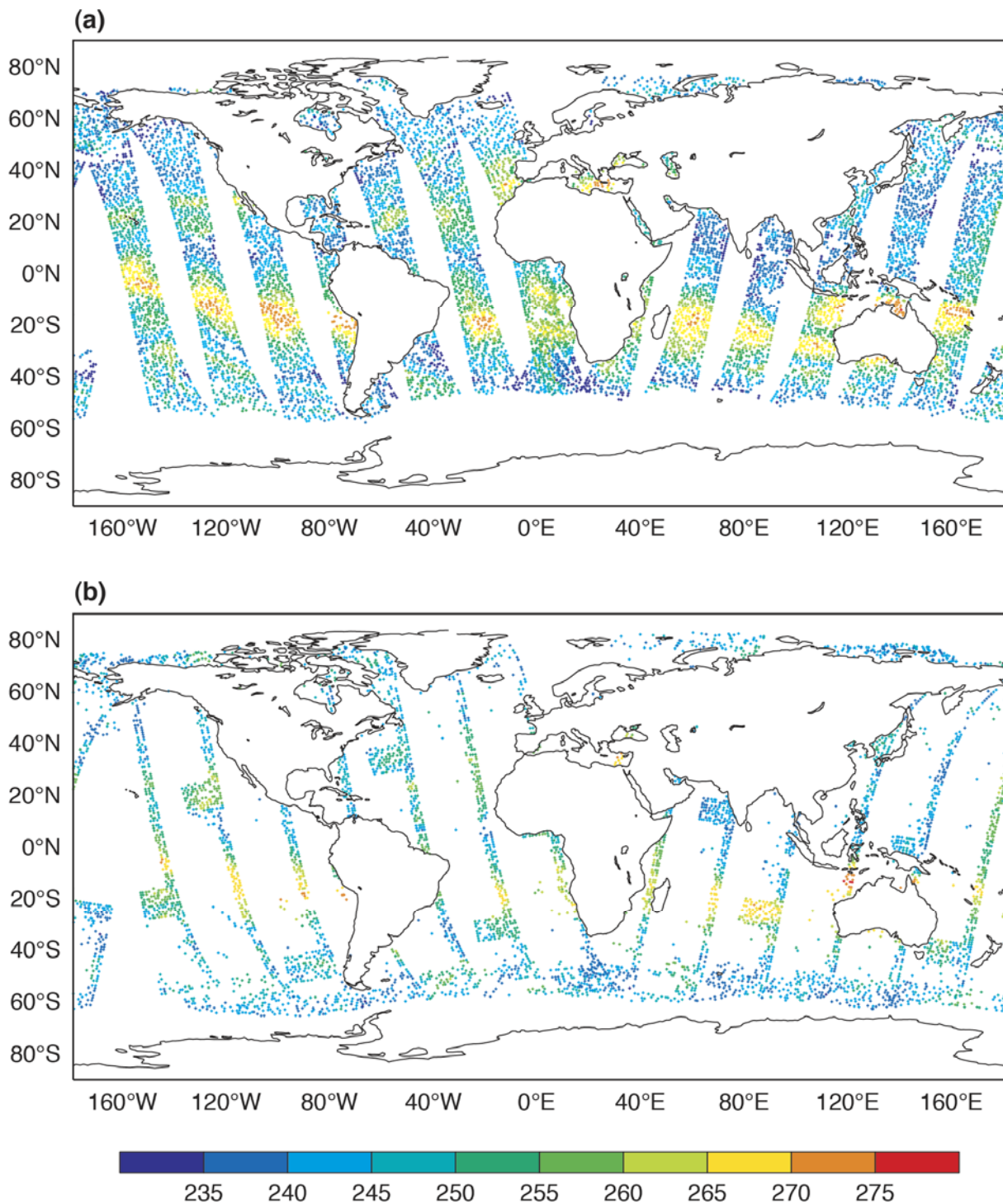


Figure 6. The 6-hour sample distributions at 00Z, August 10th, 2013; (a) of MHS, (b) of MWHS.

Departure statistics for MWHS have also been evaluated as a function of scan-position, to further evaluate the performance of the bias correction, following reports by Lu et al. (2011b) of significant scan-position-dependent biases for the FY-3A MWHS. The periods September 1st to September 10th, 2013 and August 29th to September 7th, 2013 were chosen for MWHS/FY-3A and MWHS/FY-3B, respectively, when the performance of the variational bias correction has stabilised. Averaged first-guess departure and standard deviation of each scan-position over the 10 days are calculated for MWHS and

MHS. As illustrated in Figure 7, the first-guess departures of MHS of each scan-position are very smooth, while the MWHS first-guess departures vary with the scan-position. The scan bias variation of MWHS/FY-3A (Figure 7a) is much larger than that of MWHS/FY-3B (Figure 7b) and their patterns do not change with time (not shown). The first guess departures of channel 5 from both instruments vary the most compared with the other two channels (not shown). Scan-biases in the ECMWF system are modelled as part of the variational bias correction through a 3rd order polynomial in the scan-position, and it is clear that this polynomial is not able to fully correct for the complex scan-position dependence of the bias for MWHS. It would be possible to reduce the residual scan-biases by introducing a separate offset for each scan-position in the bias correction. However, given the size of the residual biases this was not considered a priority. The averaged standard deviation of each scan-position of MWHS is also larger than that of MHS, which is consistent with our study mentioned above. This also shows that the residual scan-position-dependent biases are not sufficient to explain the larger standard deviations over all scan-positions.

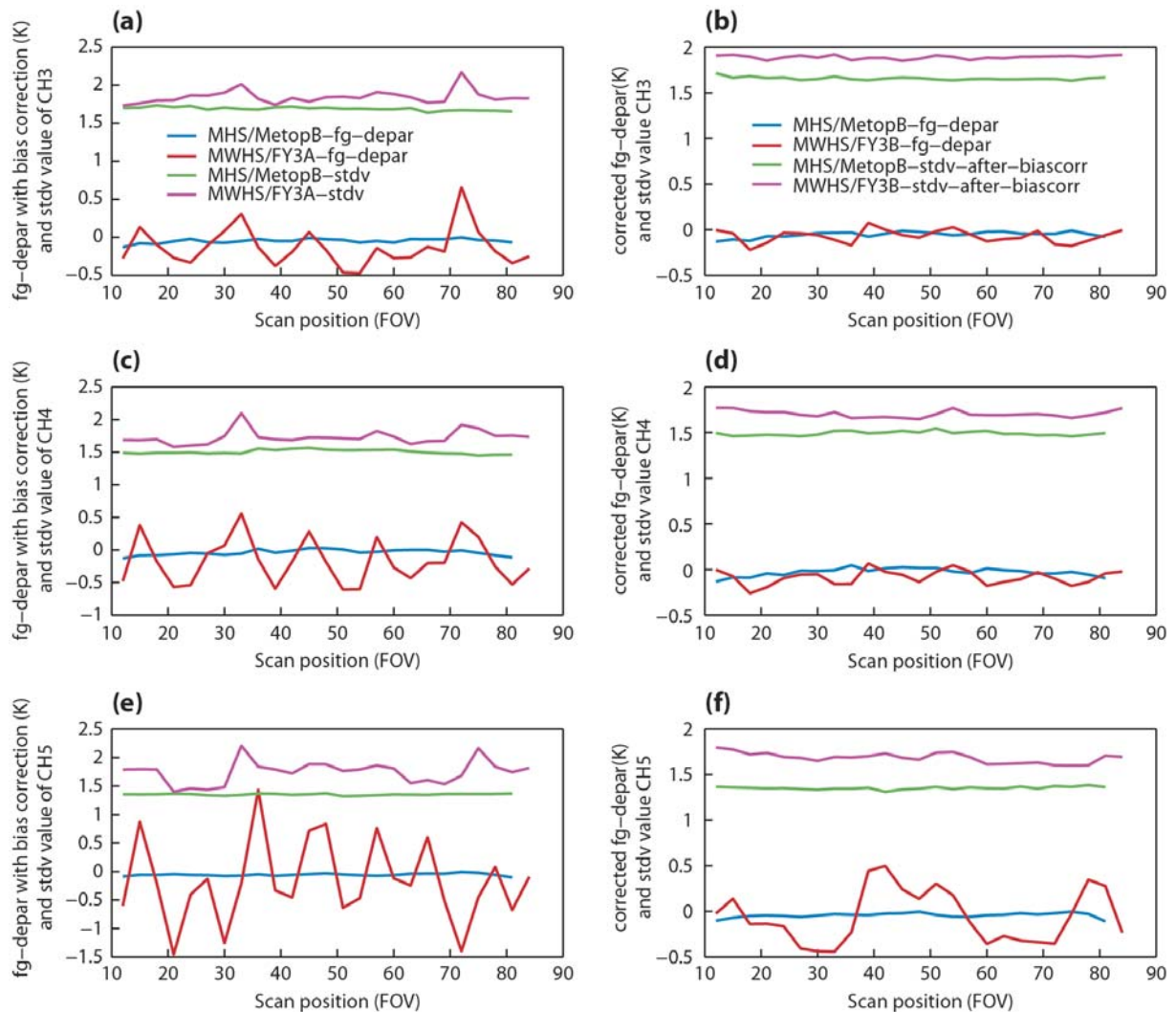


Figure 7. First-guess departures and standard deviations of each used scan-position of MWHS and MHS. (a), (c), (e) MWHS/FY-3A vs MHS of CH3, CH4, CH5, respectively; (b), (d), (f) MWHS/FY-3B vs MHS of CH3, CH4, CH5, respectively. ‘*’ is for MWHS and ‘+’ is for MHS.

4.3 Analysis impacts

Departure statistics for other observations show that the assimilation of MWHS data does not degrade the performance of the assimilation system. Globally, it decreases the standard deviation of the first-guess and analysis departures (O-B) of MHS (Figure 8). Similar improvements were found over the Northern Hemisphere, Southern Hemisphere and Tropics, respectively (not shown). Even better results are obtained by assimilating MWHS/FY-3A and MWHS/FY-3B together (Figure 8). The black line is for the combination of both MWHS instruments and the red line is for the FY-3A or FY-3B instrument individually. The standard deviations of the first-guess departure (O-B) and analysis departure of MHS are reduced more with the combination of both instruments than when only one is used.

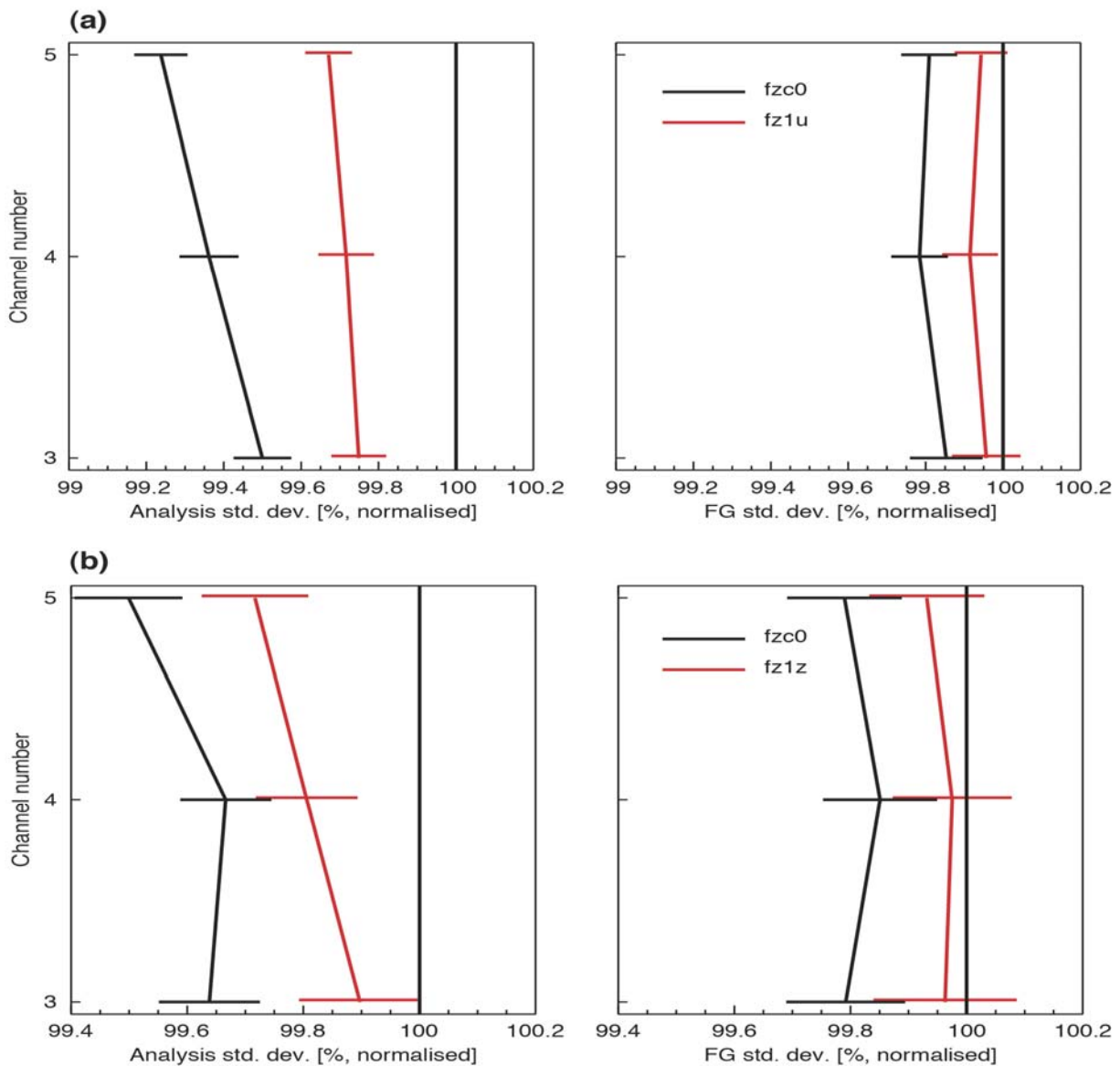


Figure 8. Standard deviations of analysis departures (left) and first-guess departures (right) of used MHS data, normalised by values for the control experiment. Horizontal bars indicate 95% confidence intervals. (a) Assimilation of the FY-3 series combination (black) vs. FY-3A/MWHS (red) and (b) FY-3 series combination (black) vs. FY-3B/MWHS (red).

4.4 Forecast assessment

The impact on the forecast of assimilating MWHS on FY-3 has also been evaluated. The forecast scores show positive results with the MWHS/FY-3A and the combined FY-3 series assimilated in the Northern Hemisphere, and are found to be neutral in the Southern Hemisphere and Tropics separately (Figure 9), while more neutral results come from the assimilation with MWHS/FY-3B (not shown). The scores are verified against both the ECMWF operational analysis and observations with similar results. The forecast error change at a range of forecast ranges, latitudes and altitudes is shown in Figure 10. Only the plots of the vector wind are shown here, as this is one of the key forecast variables known to have sensitivity to humidity assimilation in 4D-var. Positive impacts are displayed in blue. Forecast errors are decreased more in both hemispheres when both MWHSs are assimilated. In the Southern Hemisphere and the Tropics, both decreased forecast errors and increased forecast errors are seen. It is noticed that the increased forecast errors are very significant around the region of 30° South. This degradation is more noticeable for FY-3B than for FY-3A (not shown).

10-Jul-2013 to 10-Sep-2013 from 106 to 125 samples. Confidence range 95%. Verified against 0001.

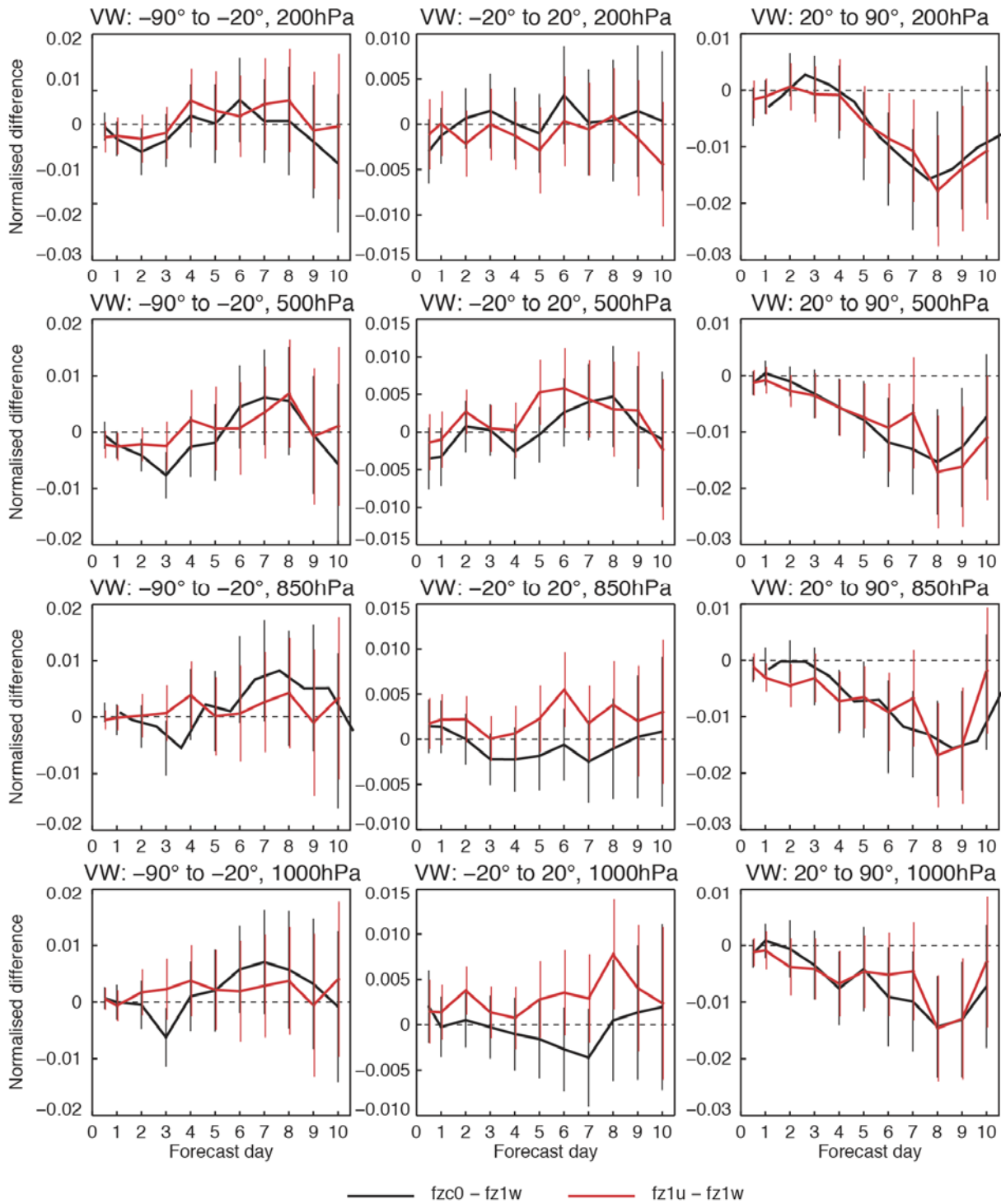


Figure 9. Ten-day forecast scores of the vector wind at different vertical levels in Northern Hemisphere, Tropics and Southern Hemisphere with MWS/FY-3B assimilated only (red line) and with both MWS/FY-3A and MWS/FY-3B assimilated (black line). Negative normalised difference means forecasting improvement at 95% confidence range.

Since the increased forecast errors are largest between 600hPa and 400hPa in Figure 10, forecast error maps at 500hPa at a range of forecast times are shown in Figure 11. Increased forecast errors are found in the Southern Hemisphere. These errors can be traced back to analysis changes in the Tropics. Therefore, the forecast errors start from the Tropics, mainly spread southward, and grow stronger with time. In order to reduce the forecast errors, tighter quality control (QC) may well be needed in the Tropics and future work will be done to investigate this.

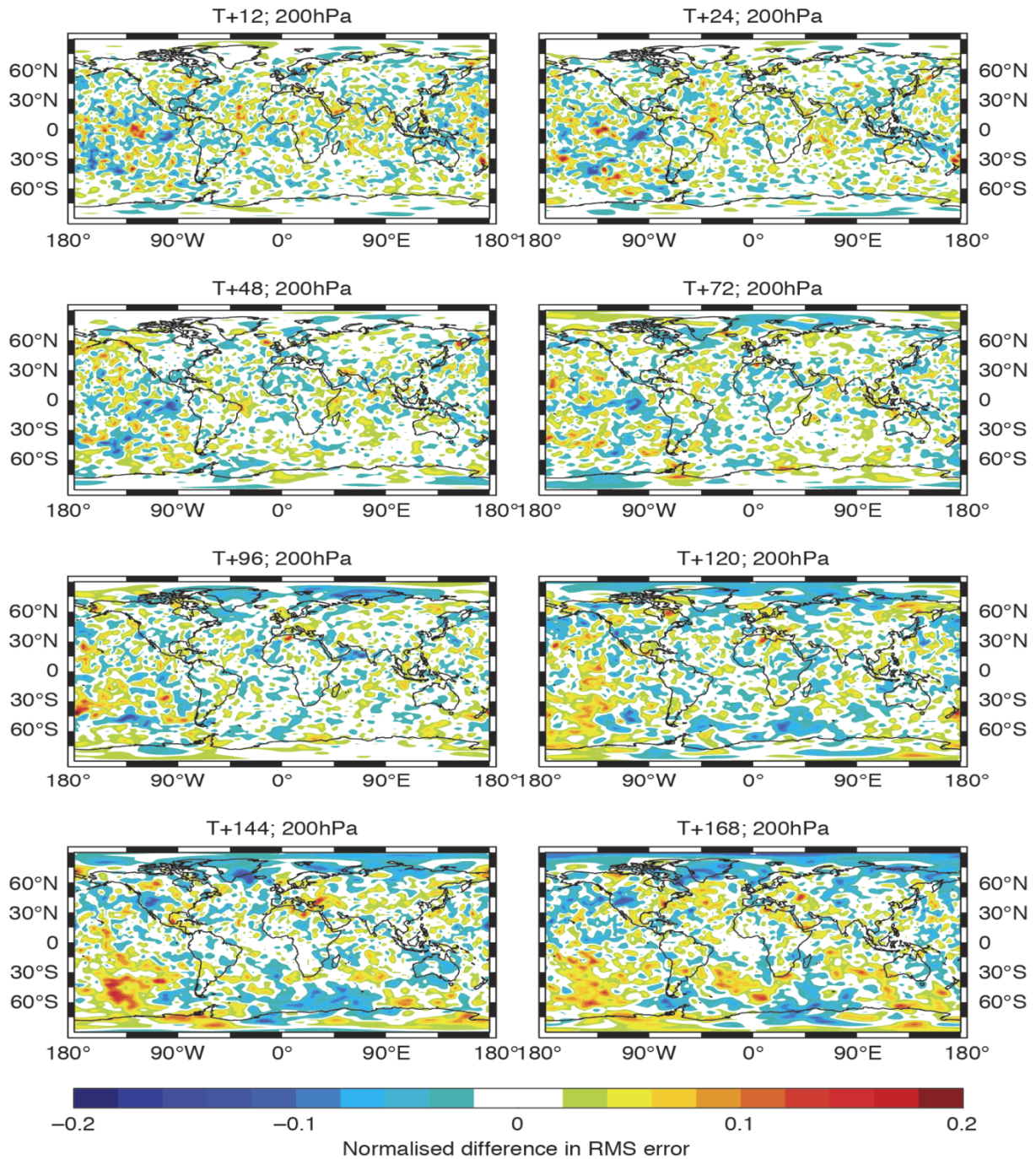


Figure 10. Maps of normalised differences in the vector wind forecast errors at 500hPa with time between MWS/FY-3B assimilated and the control. Blue indicates the reduced forecast errors.

4.5 Winter trial

Since all the experiments above are run during the Northern Hemisphere summer, the experiments need to be repeated in the Northern Hemisphere winter to understand if differences between the hemispheres are a seasonal effect. Another three experiments are run for the winter trial. The assimilation of the control run (Exp ID is g3u9) still matches the ECMWF full operational system on the selected period from December 1st, 2013 to February 28th, 2014. The forecast times are 00Z and 12Z each day, which produces 180 forecast samples in total. This experiment group used ECMWF Cycle 40r2 with a T511 spectral truncation, providing a spatial resolution of about 40km. One experiment added MWHS/FY-3B clear data over sea only (ID g3w8), and the other one added both MWHS/FY-3A and MWHS/FY-3B clear data over sea into the assimilation system (ID g3ug). Both experiments have the same period as the control run.

Consistently, with the assimilation of MWHS, the standard deviation of the first-guess and analysis departures of MHS are reduced globally (Figure 11a) and similar positive impacts are shown in both hemispheres and Tropics (not shown). Surprisingly, the reduction is larger when assimilating MWHS/FY-3B only, which is in contrast to the results for the July–September experiments. But the standard deviation of the analysis departures are always improved more with two MWHS instruments.

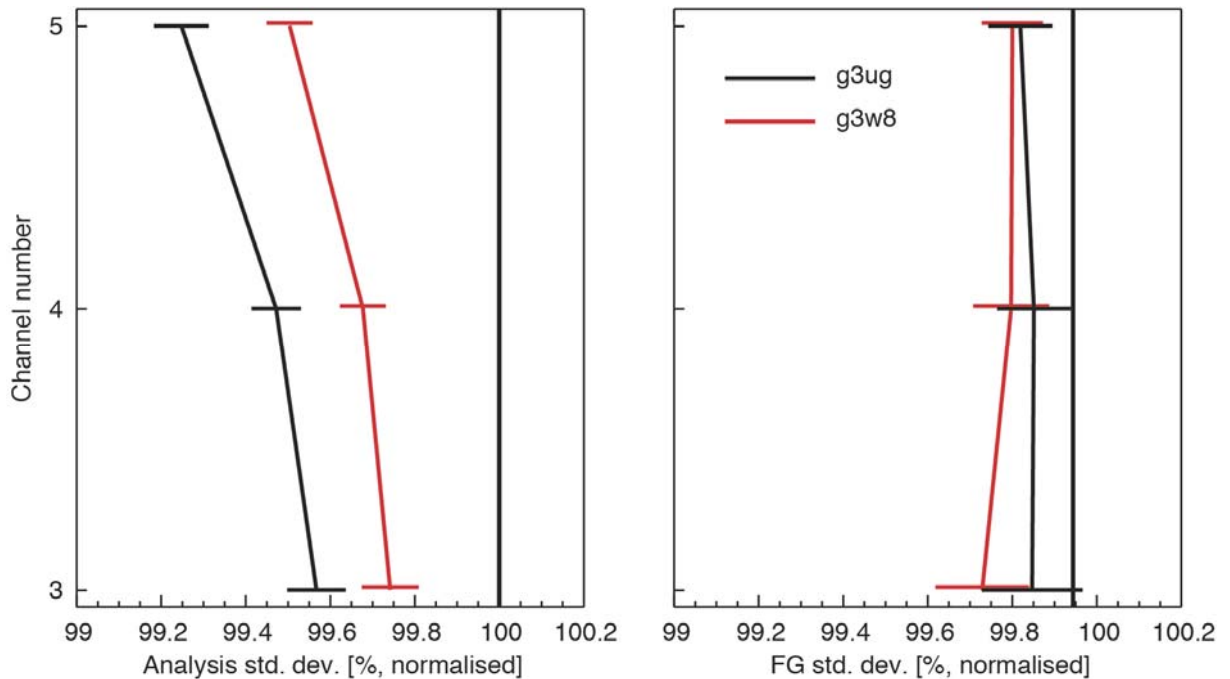


Figure 11. The normalised standard deviation of the first-guess departures and the analysis departures of MHS after assimilation with FY-3 series combination (black line) vs that with FY-3B/MWHS input (red line) in winter trials.

1–Dec–2013 to 23–Feb–2014 from 150 to 169 samples. Confidence range 95%. Verified against 0001.

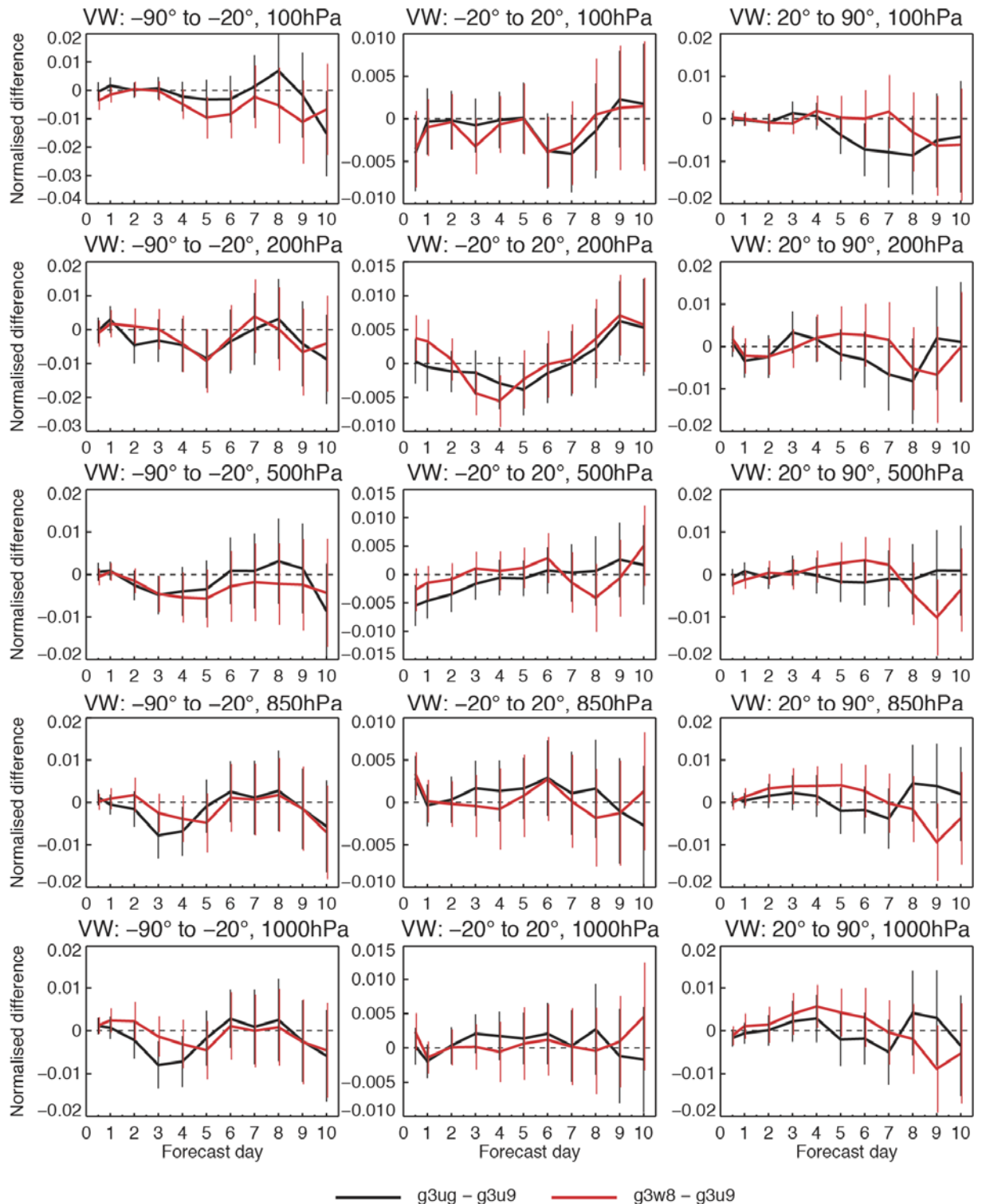


Figure 12. Ten-day forecast scores of the vector wind at different vertical levels in Northern Hemisphere, Tropics and Southern Hemisphere with MWSH/FY-3B assimilated only (red line) and both MWSH/FY-3A and MWSH/FY-3B assimilated (black line) in winter trial. Negative normalized difference means forecasting improvement at 95% confidence range.

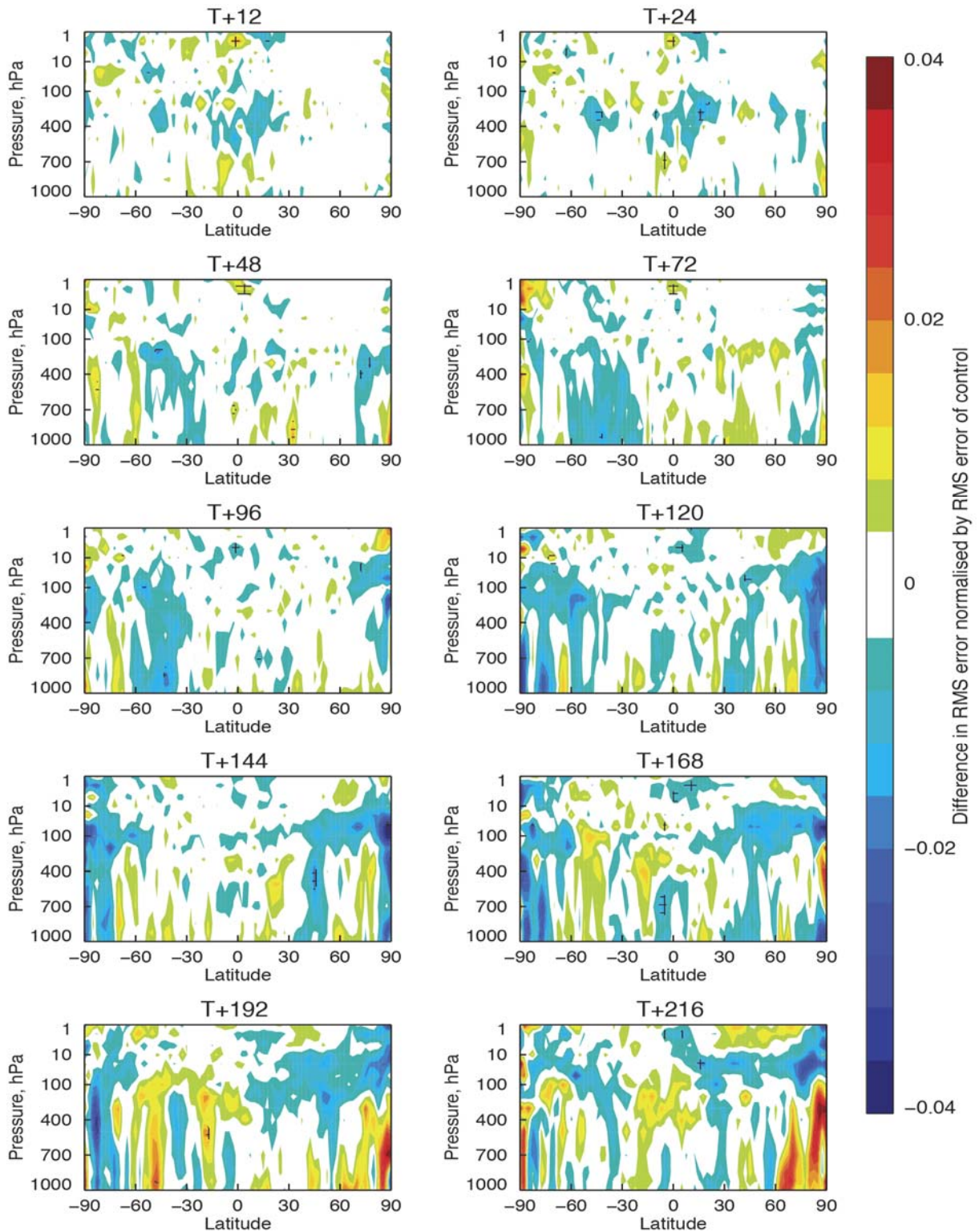


Figure 13. Zonal means of the difference in forecast errors of the vector wind with time between the experiment with both MWSH/FY-3A and MWSH/FY-3B assimilated and the control, normalized by the errors in the control. Cross-hatching indicates 95% confidence. Blue indicates reduced forecast errors. The period covered is 1 December 2013–23 February 2014.

The forecast impacts in the winter trials are also evaluated, and the forecast scores and errors are verified against the ECMWF operational analysis and observations. The winter trial forecast scores show more neutral impacts globally and for each hemisphere with the assimilation of MWHS/FY-3B only and the combined FY-3 series, respectively (Figure 12). Consistent results are obtained with enhanced positive forecast impacts in both hemispheres when two MWHSs are assimilated (Figure 13). Smaller negative impact patches are mainly shown over the Tropics and the region close to the polar area.

4.6 Overall impacts for two seasons

To further evaluate the overall impacts over both seasons, Figure 14 shows combined results for the summer and winter trials, providing 305 samples in total. Globally, assimilating one or two MWHS instruments has similar positive impact to improve the MHS first-guess departures and slightly better results from assimilation of MWHS/FY-3B only are shown in the Northern Hemisphere, but not in the Southern Hemisphere and Tropics (not shown). The reason that the results from the combined FY-3 series are not significantly better than from a single MWHS instrument might be that the number of MWHS/FY-3A used data is about 30% less than that of MWHS/FY-3B. Therefore, the increase in the number of assimilated MWHS data is smaller when MWHS/FY-3A is added on top of MWHS/FY-3B, resulting in a smaller additional impact. The combined FY-3 series nevertheless leads to the better fit for analysis departures, which suggests good consistency between these observations when more data is input.

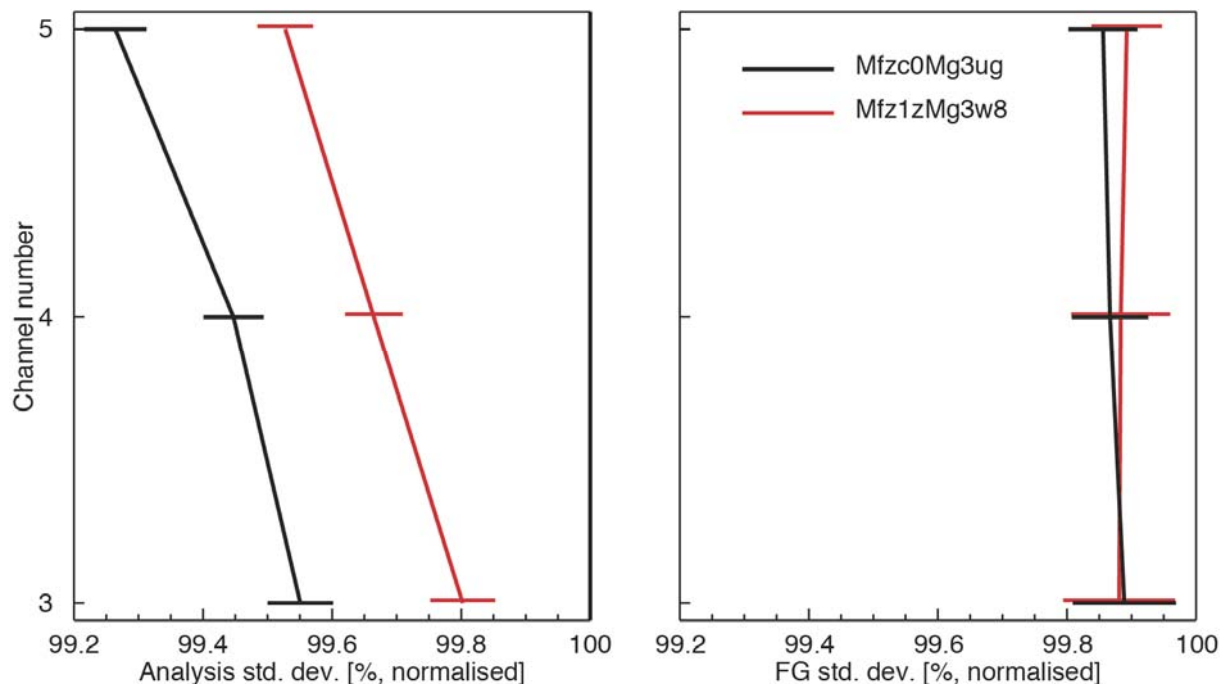


Figure 14. The normalised standard deviation of the first-guess departures and the analysis departures of MHS after assimilation with FY-3 series combination (black line) vs that with FY-3B/MWHS input (red line) in merged trials.

Over both seasons combined, MWS shows more positive forecast impacts in the Northern Hemisphere, but gives quite neutral results in the Southern Hemisphere and the Tropics (Figure 15). When two MWS are assimilated, the positive forecast impact is enhanced (Figure 15).

10-Jul-2013 to 28-Feb-2014 from 260 to 298 samples. Confidence range 95%. Verified against own-analysis.

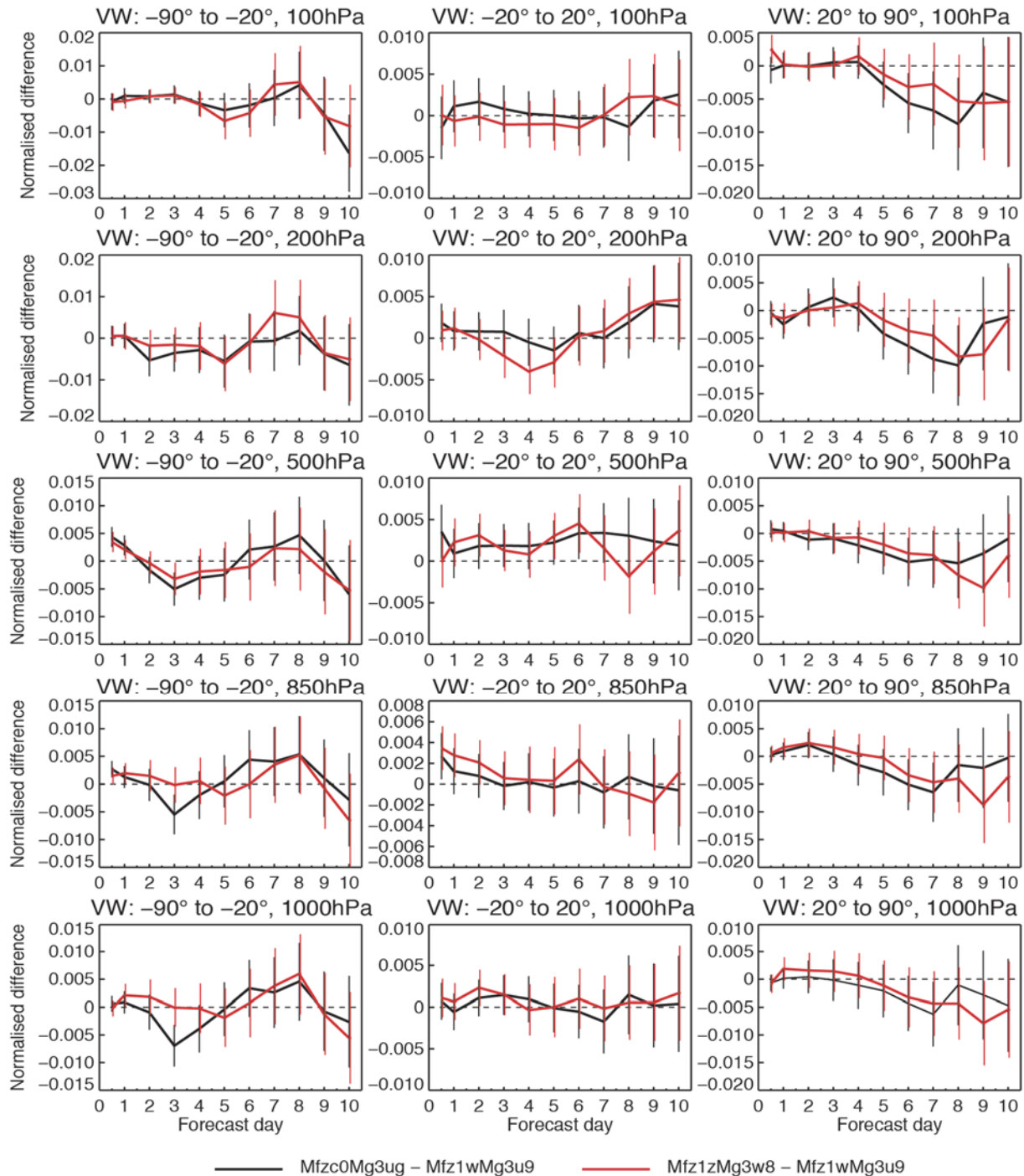


Figure 15. Ten-day forecast scores of the vector wind at different vertical levels in Northern Hemisphere, Tropics and Southern Hemisphere with MWS/FY-3B assimilated only (red line) and both MWS/FY-3A and MWS/FY-3B assimilated (black line) in the merged experiments. Negative normalized difference means forecasting improvement at 95% confidence range.

5 Substitution experiments

The trials above show the positive impacts from MWHS on the forecasting system when the data is used on top of the full operational observing system. To further characterise the impact of MWHS in comparison to MHS, we now study the respective impact of the two instruments when they are added to a depleted observing system without MHS or MWHS data. Our baseline experiment (EXP ID g3zg) uses all operational observations except MHS. Two groups of substitution experiments are set up to compare the forecasting capability of MWHS and MHS. In the first group, MWHS/FY-3A and MWHS/FY-3B clear data over sea is assimilated in the experiment g3zh and MHS data over sea from Metop-B and NOAA-18 is activated in the experiment g3zi. The other group assimilates MWHS/FY-3B clear data over sea only (EXP ID g40j), corresponding to the assimilation with MHS/NOAA-18 data over sea (EXP ID g40i) to detect the forecasting capability of a single instrument. Table 4 shows the equatorial crossing time (ECT) of the FY-3 series, Metop-B and NOAA-18. The Metop-B and NOAA-18 satellites were chosen for the MHS experiments, as their ECT is closest to that of FY-3A and FY-3B, respectively.

Satellite	ECT	Satellite	ECT
FY-3A	10:15 desc	Metop-B	09:30 desc
FY-3B	13:40 asc	NOAA-18	15:23 asc

Table 4. Satellites and their equatorial crossing time (ECT).

Forecast scores and errors are evaluated by verifying against operational analyses. Overall, the forecast scores from the assimilation of the MWHS/FY-3 series and the assimilation of MHS/Metop-B and NOAA-18 are comparable for most geophysical parameters. Even better results from the former (red line) can be seen for the Southern Hemisphere and the higher level of the Northern Hemisphere (Figure 16). The forecast error change of the vector wind at a range of forecast times, latitudes and altitudes is shown in Figure 17 with improvement displayed in blue. Forecast errors are reduced globally with assimilation of MWHS/FY-3 series, which is comparable to the improvement from the assimilation of the two MHS for the day-2 forecast and beyond. For the short-range forecasts, MHS appears to give better results, although some of this may be due to MHS being included in the operational analyses used here for verification. The results verified against observations further show that the assimilation of MWHS/FY-3 series brings positive impacts on the baseline as well as the assimilation of MHS instruments does. As for the performance of a single instrument, similar conclusions can be drawn by comparing the assimilation of MWHS/FY-3B and MHS/NOAA-18 separately (not shown).

1–Dec–2013 to 23–Feb–2014 from 150 to 169 samples. Confidence range 95%. Verified against 0001.

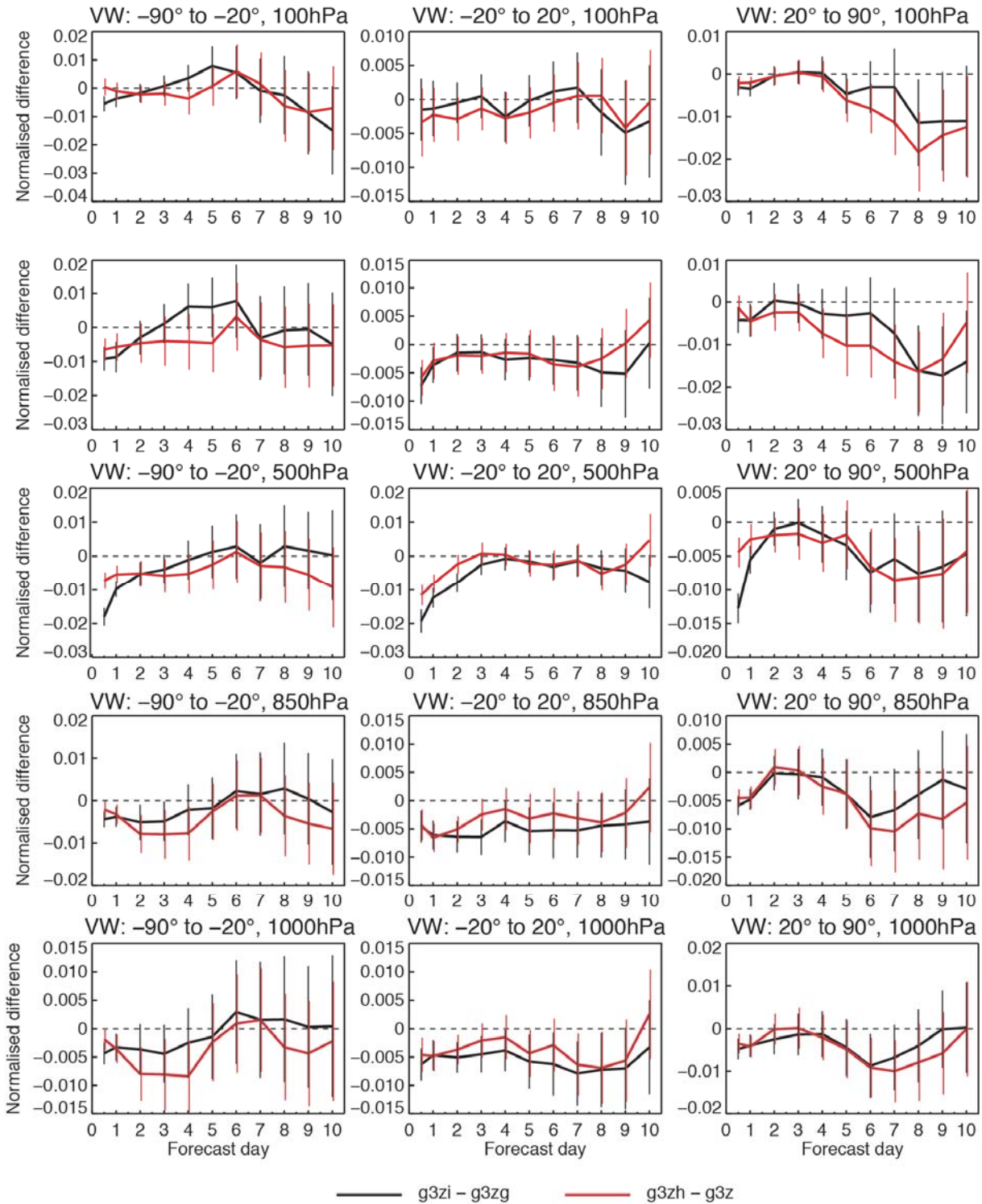


Figure 16. Ten-day forecast scores of the vector wind at different vertical levels in Northern Hemisphere, Tropics and Southern Hemisphere with assimilation of MWS/FY-3 series data over sea (red line) and MWS data over sea of Metop-B and NOAA-18 (black line) separately. Negative normalized difference means forecasting improvement at 95% confidence range.

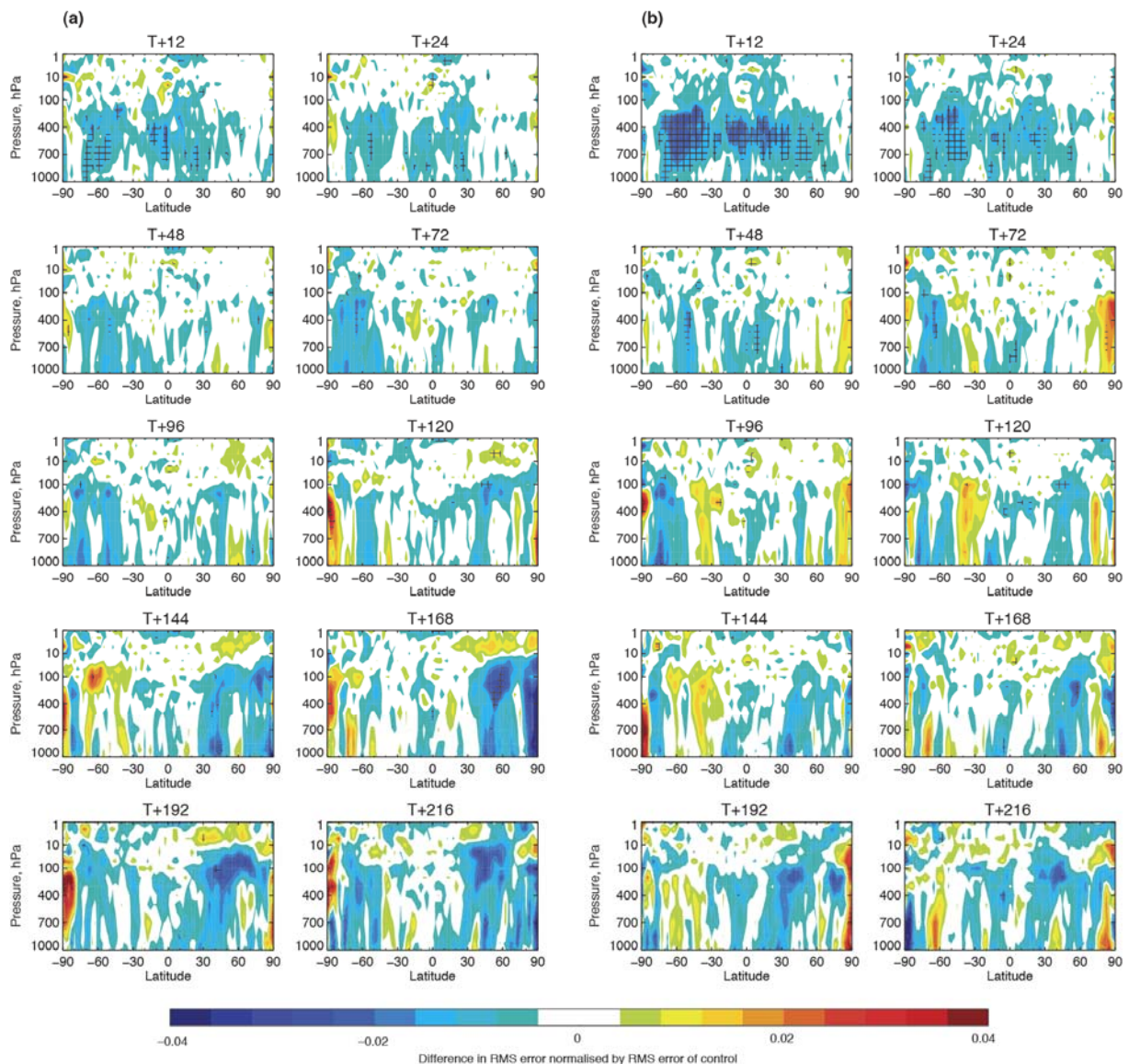


Figure 17. (a) Zonal means of the difference in forecast errors of the vector wind with time between the experiment with both MWSH/FY-3A and MWSH/FY-3B data assimilated and the baseline experiment, normalised by the baseline experiment. (b) As (a), but for the normalised difference in forecast errors between the experiment with MWS data from Metop-B and NOAA-18 and the baseline experiment. Cross-hatching indicates 95% confidence. Blue indicates reduced forecast errors. The period covered is 1 December 2013 to 23 February 2014.

6 Conclusions

Data from the microwave humidity sounding instruments on the FY-3 satellites has been tested in the ECMWF Integrated Forecasting System (IFS). This permits both an assessment of data quality through an analysis of first-guess departure statistics compared with the equivalent MetOp-B instruments, as well as evaluation of the potential impacts on operational forecasts through data assimilation experiments. The first-guess departure statistics indicate that MWSH data has higher noise than MWS data. There are also occasional calibration issues seen in first-guess departures that in the period studied here were removed successfully by quality control, but need to be understood. This demonstrates that

more monitoring of the calibration should be done during the ground processing. Averaged first-guess departure patterns by scan-position show relatively complex bias characteristics as a function of scan-position that are not fully removed by our current approach to bias correction. This suggests that a small benefit could be achieved through an improved bias correction of these aspects.

The data quality assessment by the assimilation experiments and operational forecasts provides valuable information on the impacts of the data on numerical weather prediction analysis and forecast scores. In the experiments presented here, the MWHS instruments were able to indicate neutral to slightly positive impact not only on humidity but also on the forecasts of vector winds. The forecast errors in both Northern and Southern Hemisphere extra-tropics are reduced more than in the Tropics. Improvements are larger when two MWHSs are assimilated (FY-3A and FY-3B) than when only one is used. Some increased forecast errors are found to originate from changes in the Tropical analysis, but the quality control still appears to be adequate for a successful assimilation of MWHS. The small degradation for the summer trial may indicate that there could be benefits from a better quality control (or possibly improvements in other aspects of the assimilation settings for MWHS), but this result was not statistically significant.

When added to a baseline system with no MHS or MWHS data, MWHS can achieve a large proportion of the impact of adding a similar number of MHS instruments in similar orbits. This further confirms that MWHS adds additional robustness to the observing system.

The data from the MWHS on the FY-3 series has given a promising impact on the NWP forecasting quality.

7 Acknowledgments

This work is also supported by China's Research and Development Special Fund for Public Welfare Industry (Meteorology GYHY(QX)200906006), which provides part of the travel funds. The authors would like to thank many people for the help with this work: Qifeng Lu from the National Satellite Meteorological Center of CMA for implementation of FY-3 data in IFS, the bias correction contributions and the data assessment of FY-3A; Heather Lawrence, Cristina Lupu and Alan Geer for all kinds of help.

8 References

- Dee, D., 2004. Variational bias correction of radiance data in the ECMWF system. In Proc. *ECMWF Workshop on Assimilation of High Spectral Resolution Sounders in NWP*, 28 June–1 July, 2004, 97–112.
- Lu, Q., Bell, W., Bauer, P., Bormann, N. and Peubey, C., 2011a. Characterizing the FY-3A microwave temperature sounder using the ECMWF model. *J. Atmos. Oceanic Technol.*, **28**, 1373–1389.
- Lu, Q., Bell, W., Bauer, P., Bormann, N. and Peubey, C., 2011b. An evaluation of FY-3A satellite data for numerical weather prediction. *Q. J. R. Meteorol. Soc.*, **137**, 1298–1311, DOI:10.1002/qj.834.

Saunders, R., Matricardi, M. and Brunel, P., 1999. A fast radiative transfer model for assimilation of satellite radiance observations - RTTOV-5. *ECMWF Tech. Memo. No. 282*.

Zou, X., Wang, X., Weng, F. and Li, G., 2011. Assessments of Chinese Fengyun Microwave Temperature Sounder (MWTS) measurements for weather and climate applications. *J. Atmos. Oceanic Technol.*, **28**, 1206–1227.